Journal of Membrane Science and Research 6 (2020) 125-134

Journal of Membrane Science & Research

journal homepage: www.msrjournal.com

Research Paper

Gas Permeation Modeling through a Multilayer Hollow Fiber Composite Membrane

Abtin Ebadi Amooghin [*,1], Saman Mirrezaei [1], Hamidreza Sanaeepur [1], Mohammad Mehdi Moftakhari Sharifzadeh [2]

[1] *Department of Chemical Engineering, Faculty of Engineering, Arak University, Arak 38156-8-8349, Iran*
[2] *Department of Petroleum and Chemical Engineering, Science and Research Branch, Islamic Azad University, Tehran, Iran*

Article info

Received 2019-08-01
Revised 2019-10-16
Accepted 2019-10-19
Available online 2019-10-19

Keywords

Gas separation
Modeling
Permeability
Hollow fiber composite membrane
Finite element method

Highlights

- A time-dependent 2D axisymmetric model developed for a multilayer HFCM
- In this model, the porous support is first exposed to the feed gas
- Gas permeation properties of pure H_2, O_2, N_2, CH_4, CO_2 and He are investigated
- By increasing the feed stream temperature, CO_2 permeability and diffusivity increased

Graphical abstract

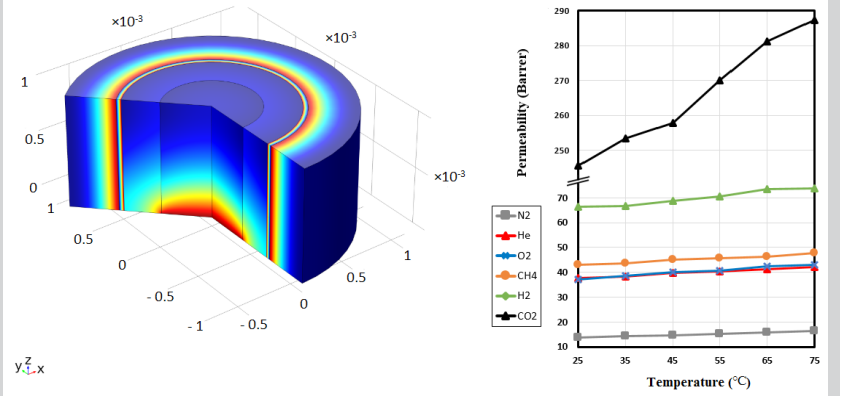

Abstract

In this study, a time-dependent 2D axisymmetric model of a multilayer hollow fiber composite membrane for gas separation is proposed. In spite of the common multilayer membranes, which a dense layer coated on a porous support layer and subjected into the feed stream, here, the porous support is exposed to the feed gas. In this regard, the governing equations of species transport are developed for model domains and then solved by a finite element method (FEM). Gas permeation properties of pure H_2, O_2, N_2, CH_4, CO_2 and He are calculated and validated with experimental data with good conformity. Obtained results indicate that with increasing the temperature, the permeability and diffusion coefficient increased while the solubility decreased. Moreover, the permeability and solubility variations with temperature for a heavier gas, CO_2, were higher than those for the lighter ones, while the diffusion coefficient variation with temperature for the lither gas, such as He, was more than the heavier ones. By increasing the CO_2 feed stream temperature from 25 to 75°C, its permeability and diffusion coefficient increased respectively from 245 to 307 Barrer and from 205 to 282×10^{-12} m^2/s, while the CO_2 solubility decreased from 0.85 to 0.76 cm3.cm3.bar1. In the case of He and for the same temperature variation range, its permeability and diffusion coefficient increased respectively from 39 to 42 Barrer and from 2180 to 2834 10^{-12} m^2/s, while the solubility of He decreased from 0.013 to 0.011 $cm^3.cm^{-3}.bar^{-1}$.

1. Introduction

Industrial progress, an increase in machinery and development of electrical power plants have enhanced the fossil fuel consumption and the consequent emission of greenhouse gases such as CO_2 and CH_4 in the atmosphere which may have destructive impacts on the environment, global warming and reducing the efficiency of related processes [1-5]. Therefore, the need for elimination of greenhouse gases has gained considerable importance along with the development of gas refinery, processing, and transport as well as the introduction of new technologies in gas separation [6, 7].

In this regards, different technologies for gas separation such as adsorption, cryogenic distillation, absorption, and spray towers have been applied [8]. These methods suffer from several drawbacks such as flooding, foaming, and channeling [9, 10]. To overcome these circumstances, membrane technology can be used which has a better operating performance, as well as low operation and energy costs [11]. Many efforts have been made to create unique materials or structures with a better ability to improve the membrane performance [12-15]. Various membrane modules such as hollow fiber, tubular, plate and frame and spiral wound have been developed. Hollow fiber membrane (HFM) is one of the most applied membrane modules. High

* Corresponding author at: Phone/fax: +98 86 32625410
E-mail address: a-ebadi@araku.ac.ir (A.Ebadi Amooghin)

DOI: 10.22079/JMSR.2019.112328.1281

surface area per unit volume is a reason for high efficiency of the hollow fiber configuration [16]. Qi and Cussler [17] are the first researchers who have used the porous polypropylene HFM for the absorption of CO_2 by using the chemical absorbent. They studied the overall mass transfer coefficients and compared the HFM performance with the packed towers.

Because of the problems and constraints in membrane construction, modeling of membrane processes is important for evaluating and predicting membrane performance under different operating conditions. Ebadi Amooghin et al. [18] proposed a mathematical model for mass transfer of multi component-gas mixture through a synthetic polymeric membrane. They introduced a new mathematical method for calculation of permeability for three-component gas through a composite membrane. Moreover, they developed a new model for direct calculation of diffusion coefficient and showed that with increasing temperature, permeability is affected. This behavior is different for the various gases. With increasing the temperature, permeability increases for H_2 and CH_4, while it decreases for C_3H_8. Darabi et al. [19] presented a comprehensive 2D mathematical model to estimate the increase of CO_2 absorption by filler incorporation in a HFM. The effect of filler loading on mass transfer increment across the membrane is justified by Brownian motion and the Grazing effect. Their results showed that incorporating of 0.05 wt.% of silica nanoparticles can enhance the absorption rate about 16%, while adding the same amount of carbon nanotube (CNT) nanoparticles, the absorption rate increases up to 32%. The CNT nanoparticle had better performances due to its high absorption and hydrophobicity relative to silica nanoparticles. The addition of CNT nanoparticles with 0.03 wt.% resulted in the highest CO_2 absorption in the HFM. Hosseini et al. [20] presented a mathematical model for mixed gas permeation (CO_2 and CH_4) in symmetric HFM. The governing equations of the model were solved by using the finite element method (FEM). The effect of pressure and temperature on CO_2/CH_4 separation performance, respectively by using the immobilization- and Arrhenius-type equations, was examined. The obtained results showed that permeability increases with increasing temperature and decreasing pressure. Farjami et al. [21] proposed a model for CO_2 elimination in polyvinylidene fluoride (PVDF) HFM in which distilled water is used as the liquid sorbent in non-wetting condition. The model was solved by the computational fluid dynamics (CFD) method. They investigated the changes in CO_2 elimination performance by liquid sorbent velocity, fiber length, membrane porosity, and liquid sorbent temperature. All of these parameters, except for the liquid sorbent temperature, had an increasing effect on CO_2 elimination performance. Tantikhajorngosol et al. [22] presented a 2D mathematical model for two HFMs and evaluated the physical absorption of CO_2, H_2S, and CH_4 from high-pressure synthetic biogas. They assumed that Henry's constants are dependent on pressure and temperature. Since H_2S is a polar gas, its polarization was also considered to be effective in H_2S diffusivity. The effect of temperature and pressure on CO_2 and H_2S absorption and also for CH_4 loss is examined. The results indicated that the rate of adsorption increases with increasing the pressure and decreasing the temperature. In this case, the amount of CH_4 loss is lower than 5.50%. Moreover, their results showed that in high pressures and non-wetting mode, PTFE membrane leads to better results such as more absorption rate of gases from biogas, while in partially wetting mode, the results of PVDF membrane had a good conformity with experimental data. Azari et al. [23] proposed a numerical model of mass transfer in a HFM in non-wetted and partially-wetted conditions for the separation of CO_2 from CO_2/N_2 mixture. Mono-ethanol-amine (MEA), 2-amino-2-methyl-1-propanol (AMP) and NaOH were used as the sorbents. The effects of porosity, temperature, fiber radius, and solvent flow rate in the model performance were investigated. The results revealed that by increasing the gas flow rate, CO_2 removal is reduced and its concentration in the outlet is enhanced. Also, by increasing the solvent flow rate and temperature, the concentration of CO_2 at the outlet is decreased. Moreover, the membrane porosity enhancement and increase of the internal radius of the fiber lead to further elimination of CO_2. Talaghat et al. [24] proposed a mathematical model for countercurrent gas-liquid flow in axial/radial directions and at fully-wet condition in polypropylene HFM contactor which applied in the removal of CO_2 from the CO_2/CH_4 gas mixture. The model equations were solved by using the COMSOL Multiphysics software. The MEA and methyl diethanolamine (MDEA) were utilized as absorbents. The results showed that MEA leads to higher CO_2 removal. Also, by increasing porosity-to-tortuosity ratio, fluid flow, the number of fibers, membrane length and solvent concentration, CO_2 removal was increased, while it decreased by increasing the gas flow rate or decreasing the contact time. Moreover, polypropylene HFM with MEA as the absorbent has higher CO_2 removal from PVDF and PTFE HFMs. In another work, a mathematical model to evaluate the separation of binary gas mixtures (CO_2/CH_4) in a HFM was presented by Dehkordi et al. [25]. The SRK and Joule-Thomson equations are used to predict non-ideal behavior and temperature variations in permeation of gas components. Also, the effect of temperature on the permeation was justified by the Arrhenius equation. The effect of physical variables such as fiber inner diameter, effective fiber length, module diameter, and the number of fibers on the model performance was also examined. The results indicated that the number of fibers and their effective length have a great effect on the gas separation. Also, by decreasing the effective length and number of fibers, the higher gas separation efficiency is achieved. Sharifzadeh et al. [26] developed a time-dependent mathematical model to study the separation of a gas mixture consist of CO_2 and N_2 through facilitated transport membranes (FTMs) which were composed of a porous polyvinyl alcohol (PVA) membrane filled with different amounts of diethanolamine (DEA). The model considered unequal diffusion coefficient for all carriers and complexes, and also a constant equilibrium parameter in the chemical reaction between carriers and permeant. Moreover, they presented a method for calculating concentration-dependent diffusion coefficients of all components passing through the FTMs. In addition, the effects of carrier concentration, reversible chemical reaction kinetics, and feed partial pressure on the model performance were investigated. The results indicated that CO_2 permeability reduces with increase in the partial pressure. By increasing the concentration of carrier and the chemical reaction kinetics, CO_2 permeability firstly increases and then decreases.

In this work, a time-dependent 2D model is developed to calculate the permeability, selectivity, solubility and diffusion coefficient of various gases such as CO_2, H_2, He, N_2, O_2 and CH_4 in a hollow fiber composite membrane. Unlike the common composite membrane models, in this model the porous support layer is subjected to the feed stream and the dense selective layer is placed on the opposite direction, the permeate side. The governing equations with related boundary conditions are developed for all zones of feed side, porous support, dense membrane, and permeate side and solved using the finite element method. In addition, the Frisch method is used to calculate the diffusion coefficient of gas components through the membrane. Additionally, the effect of temperature on gas permeation properties is investigated.

2. Model development

2.1. Theory

A time-dependent 2D axisymmetric model was developed for a hollow fiber composite membrane which is composed of poly (styrene-b-butadiene-b-styrene), triblock copolymer (SBS) with a rubbery character that is coated on a polyacrylonitrile (PAN) porous support [27]. A bundle of the membrane fibers modulated in a dead end membrane holder. According to the experimental paper, in this study, in spite of the common multilayer membranes, SBS selective layer was coated on the external surface of the PAN support, and because of the porous PAN support is used only for mechanical stability, it has no important role in species transport, or in turn, in the mass transfer mechanism and the separation performance. As well as in a constant height for a fiber, its radius and consequently the membrane surface area increases. Therefore, the amounts of species transport across the membrane or the mass flow rate increase that has no considerable effects on the permeability and selectivity.

Figure 1 shows a schematic of the model zones that considers a fiber consisting four sections: feed side, porous support, dense membrane, and permeate side. Feed gas comes into the feed side (at $z = 0$) at 25 °C and 1 bar and the permeate stream exits from the opposite side of the membrane model (at $r = r_4$).

The solution-diffusion mechanism has been utilized to describe mass transfer in this model [28]. Following assumptions are considered in the proposed model:

- The diffusion mechanism is based on Fick's law.
- The gas flow arrangement in the model is radial and axial flow is neglected.
- The model is time-dependent.
- Ideal gas behavior is assumed.
- A pressure difference is a driving force in the model.
- There is no heat transport in the model.
- The laminar flow regime is considered for gas flow in the model.

2.2. Governing equations

The continuity equations in different sections of hollow fiber composite membrane are as follow [29, 30]:

$$\frac{\partial C_{i,F}}{\partial t} + \nabla.\left(-D_{i,F}\ \nabla C_{i,F}\right) = -u_{i,F}\ .\nabla C_{i,F} \quad \text{Feed side} \quad (1)$$

$$\frac{\partial C_{i,S}}{\partial t} + \nabla.\left(-D_{i,S}\ \nabla C_{i,S}\right) = -u_{i,S}\ .\nabla C_{i,S} \quad \text{Support layer} \quad (2)$$

$$\frac{\partial C_{i,m}}{\partial t} + \nabla.\left(-D_{i,m}\ \nabla C_{i,m}\right) = 0 \quad \text{Membrane} \quad (3)$$

$$\frac{\partial C_{i,p}}{\partial t} + \nabla.\left(-D_{i,p}\ \nabla C_{i,p}\right) = -u_{i,p}\ .\nabla C_{i,p} \quad \text{Permeate} \quad (4)$$

where C is the concentration (mol/m^3), D is the diffusion coefficient (m^2/s), u denotes the velocity vector (m/s) and t is time (s).

To obtain the velocity distribution and concentration gradient in both feed and permeate sections, a momentum balance by employing the Navier-Stokes equation is investigated and simultaneously solved with the continuity equations. Additionally, coupling Navier–Stokes and continuity equations together is a conventional approach in this case of membrane modeling [31-33].

The velocity distribution of gas in the feed and permeate sections is calculated by the Navier–Stokes equation as following [34, 35]:

$$\rho_i \frac{\partial u_{i,p}}{\partial t} + \rho_i\ (u_{i,p}\nabla)\ u_{i,p} = -\nabla P_{i,p} + \nabla\eta_i\left(\nabla u_{i,p}\right) + (\nabla u_{i,p})^T) + F \quad (5)$$

where P, F, η and ρ are related to pressure (Pa), external forces (N/m^3), dynamic viscosity (kg/m.s) and density of the gas (kg/m^3); respectively. r_4 is the Happle's free surface which is obtained from Eq. (6) [36]:

$$r_4 = r_3\left(\frac{1}{1-\alpha}\right)^{0.5} \quad (6)$$

α is the void volume in the module and can be expressed by Eq. (7):

$$\alpha = 1 - \frac{n r_3^{\,2}}{R^2} \quad (7)$$

where n refers to the number of fibers and R is the module inner radius.

Because of the gas fluxes in the model are defined by the stiff-spring method, the boundary condition are defined as follow:

(i) Feed side

@ r = 0 $\quad C_{i,j} = 0$ (symmetry) (8)

@ $r = r_1$ $\quad -n.N = M * (C_2 - K*C_1)$; $\quad N = -D_{i,f}\nabla C_{i,f} + C_{i,f}\,u_{i,f}$ (9)

@ Z = 0 $\quad C_{i,f} = C^0_{i,f}$ (concentration) (10)

@ Z = L $\quad n.N = 0$; $N = -D_{i,f}\nabla C_{i,j} + C_{i,f}\,u_{i,f}$ (11)

(ii) Support layer

@ $r = r_1$ $\quad -n.N = M * (K*C_1 - C_2)$; $\quad N = -D_{i,s}\nabla C_{i,s} + C_{i,s}\,u_{i,s}$ (12)

@ $r = r_2$ $\quad -n.N = M*(C_3 - K*C_2)$; $\quad N = -D_{i,s}\nabla C_{i,s} + C_{i,s}\,u_{i,s}$ (13)

@ z = 0, z = L $\quad n.N = 0$; $\quad N = -D_{i,s}\nabla C_{i,s} + C_{i,s}\,u_{i,s}$ (14)

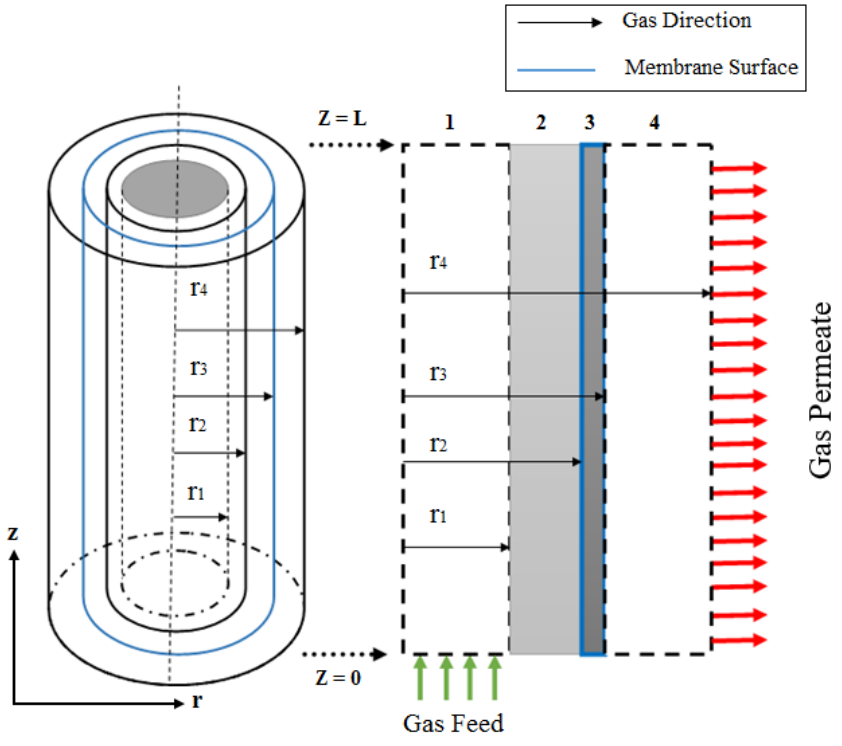

Fig. 1. Schematic of a hollow fiber composite membrane which is used in the model (Scaled in z-coordinate: 1/100).

(iii) Membrane side

$$@\ r=r_2 \qquad -n.N = M*(K*C_2 - C_3); \qquad N = -D_{i,m}\nabla C_{i,m} \tag{15}$$

$$@\ r=r_3 \qquad -n.N = M*(K*C_4 - C_3); \qquad N = -D_{i,m}\nabla C_{i,m} \tag{16}$$

$$@\ z=0;\ z=L \qquad n.N = 0; \qquad N = -D_{i,m}\nabla C_{i,m} \tag{17}$$

(iv) Permeate side

$$@\ r=r_3 \qquad -n.N = M*(K*C_4 - C_3); \qquad N = -D_{i,p}\nabla C_{i,p} + C_{i,p}u_{i,p} \tag{18}$$

$$@\ r=R \qquad -n.(-D_{i,j}\nabla C_{i,j}) = 0 \tag{19}$$

$$@\ z=0;\ z=L \qquad n.N = 0; \qquad N = -D_{i,p}\nabla C_{i,p} + C_{i,p}u_{i,p} \tag{20}$$

In addition, the boundary conditions for solving the Navier–Stokes equation in the feed and permeate sides are:

(i) Feed side

$$@\ r=0 \qquad \text{symmetry} \tag{21}$$

$$@\ r=r_1 \qquad u_{i,f} = 0 \text{ (no slip condition)} \tag{22}$$

$$@\ Z=0 \qquad P=P_0 \text{ (initial pressure)} \tag{23}$$

$$@\ Z=L \qquad u_{i,f} = 0 \text{ (no slip condition)} \tag{24}$$

(ii) Permeate side

$$@\ r=r_3 \qquad u_{i,p} = 0 \text{ (no-slip condition)} \tag{25}$$

$$@\ r=R \qquad P = 0 \text{ (vacuum)} \tag{26}$$

$$@\ Z=0;\ Z=L \qquad u_{i,p} = 0 \text{ (no-slip condition)} \tag{27}$$

where $C^0_{i,j}$, and N refer to initial concentration (mol/m^3) and total gas flux (mol/m^2.s), respectively. In this case, considering the ideal gas and by dividing the inlet pressure by RT the initial concentrations are obtained [37-40]. The stiff-spring method is employed to overcome discontinuity in concentration profile due to discontinuity in the boundaries for gas flux calculation. Therefore the Dirichlet concentration boundary condition is substitute by the continuous flux condition is defined based on the partition coefficient (K) that resolves the flux discontinuity as follow [6]:

$$N = M\left|C_{i,j+1} - K_i C_{i,j}\right| \tag{28}$$

$$K_i = \frac{C_{i,j+1}}{C_{i,j}} \tag{29}$$

where *i* and *j* are corresponded to each species and points, respectively. M is the Stiff-spring velocity (a non-physical parameter) and usually has a large amount (100,000 in this work). This parameter is employed in order to align the flux at both sides of two neighboring sections [41, 42]. K_i denotes the dimensionless partition coefficient which experimentally derived by Henry's law [43].

In order to prevent the creation of large numbers of nodes and elements due to the low thickness of the dense membrane, this section is scaled in the axial direction. Therefore, the correlating diffusion coefficient is utilized instead of the effective diffusion coefficient. The scaled z-coordinate can be defined as following [17]:

$$\bar{z} = \frac{z}{\text{scale}} \qquad (\text{scale} = 100) \tag{30}$$

The correlating diffusion coefficient matrix in each section are obtained as follows [41]:

$$D_{ij,\text{eff}} = \begin{bmatrix} \frac{D_{i,j}}{\text{scale}^2} & 0 \\ 0 & D_{i,j} \end{bmatrix} \qquad \text{zones 1 and 4} \tag{31}$$

$$D_{s,\text{eff}} = \begin{bmatrix} \frac{D_s}{\text{scale}^2} & 0 \\ 0 & D_s \end{bmatrix} \qquad \text{zone 2} \tag{32}$$

$$D_{m,\text{eff}} = \begin{bmatrix} \frac{D_m}{\text{scale}^2} & 0 \\ 0 & D_m \end{bmatrix} \qquad \text{zone 3} \tag{33}$$

The gas flux and solubility are obtained based on the Fick's law and Henry`s law, respectively [44, 45]:

$$J = -D_{AB}\frac{\partial C}{\partial r} \tag{34}$$

$$S = \frac{P_i}{D_i} \tag{35}$$

where S, $\frac{\partial C}{\partial r}$ and *P* are solubility (cm^3/cm^3.bar), concentration gradient (mol/m^4) and permeability (Barrer), respectively. The permeability can be defined as following [46]:

$$p = \frac{J \times l}{\Delta P} \tag{36}$$

where, *J*, *l* and ΔP refer to gas diffusive flux (mol/(m^2.s)), membrane thickness (m), and pressure gradient (Pa), respectively. Moreover, the ideal selectivity is calculated by the Eq. (37) [47, 48]:

$$\alpha_i = \frac{P_i}{P_{N_2}} \tag{37}$$

2.3. Time lag method

Time lag is an efficient method for evaluation of diffusivities even for the complex diffusional systems [49-54]. This method is applicable for ideal mass transfer and non-Fickian diffusion in systems. Also, it can be used for concentration, position, or time-dependent systems. Here, Frisch method is employed in order to drive the time lag, which is a main feature of diffusion mechanism [55-58]. The time lag value can be obtained by the intercept of the tangent line in the linear part of the pressure-time curve with the t-axis [29, 59].

Frisch method is used in calculating both the concentration dependent and concentration independent diffusion coefficients [49]. Here, by using this method the diffusion coefficient and the value of time lag are obtained according to the algorithm in Figure 2 [17, 60].

Based on the presented algorithm at Figure 3, in the first step physical properties and required operating conditions are defined. In the next step, Frisch method is investigated to calculate the diffusion coefficient and time lag values. Then, by using Eq. (38) [61, 62] and the derived time lag value from the p-t curve [63], diffusion coefficients are obtained.

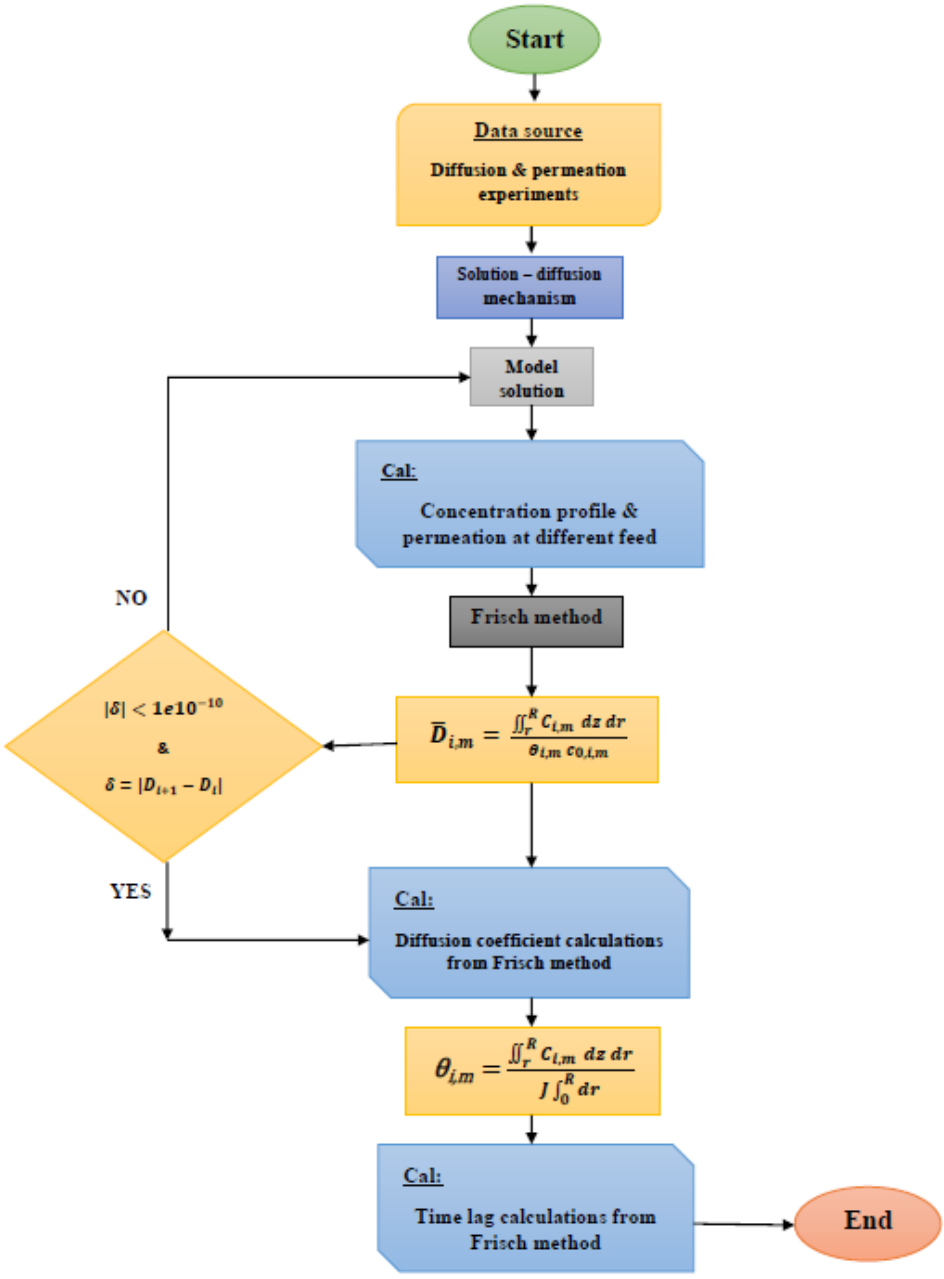

Fig. 2. Solution algorithm for calculating diffusion coefficient of a gas component.

$$\bar{D}_{i,m} = \frac{\iint_r^R C_{s,i,m}\,(r)\, dz\, dr}{\theta_{i,m}\, c_{0,i,m}} \quad (38)$$

where $C_{i,m}$ refers to the concentration distribution of penetrant gas. The solution loop is repeated as long as the desired diffusion coefficient is achieved. It is mentioned that the number of repetitions of this loop is different for each gas component. For instance, this loop was repeated up to 17 times for N_2. The time lag value can be obtained by Eq. (39) [17].

$$\theta_{i,m} = \frac{\iint_r^R C_{s,i,m}\, dz\, dr}{J\int_0^R dr} \quad (39)$$

3. Model solution

The model equations all four domains with respect to the proper boundary conditions for various gases such as H_2, O_2, N_2, CH_4, CO_2 and He were solved by finite element method. In this regard, COMSOL Multiphysics version 5.2 was utilized with Intel Core i7 CPU M 460 @ 2.60 GHz and 8 GB RAM system. Finite error analysis was combined with error control and adaptive meshing using a solver which was matched for solving boundary value problems [64, 65]. Some parameters such as pressure, temperature and diffusion coefficients in the hollow fiber composite membrane were derived from the literature [27]. The other required parameters such as diffusion coefficients in feed and permeate sections were obtained from Wilke-Lee equation [66]. The generated mesh for each of the gas components was different. As shown in Figure 3, extra fine mesh is used for H_2, N_2, O_2 and He, while it was implemented coarser mash sizes for CH_4 and CO_2.

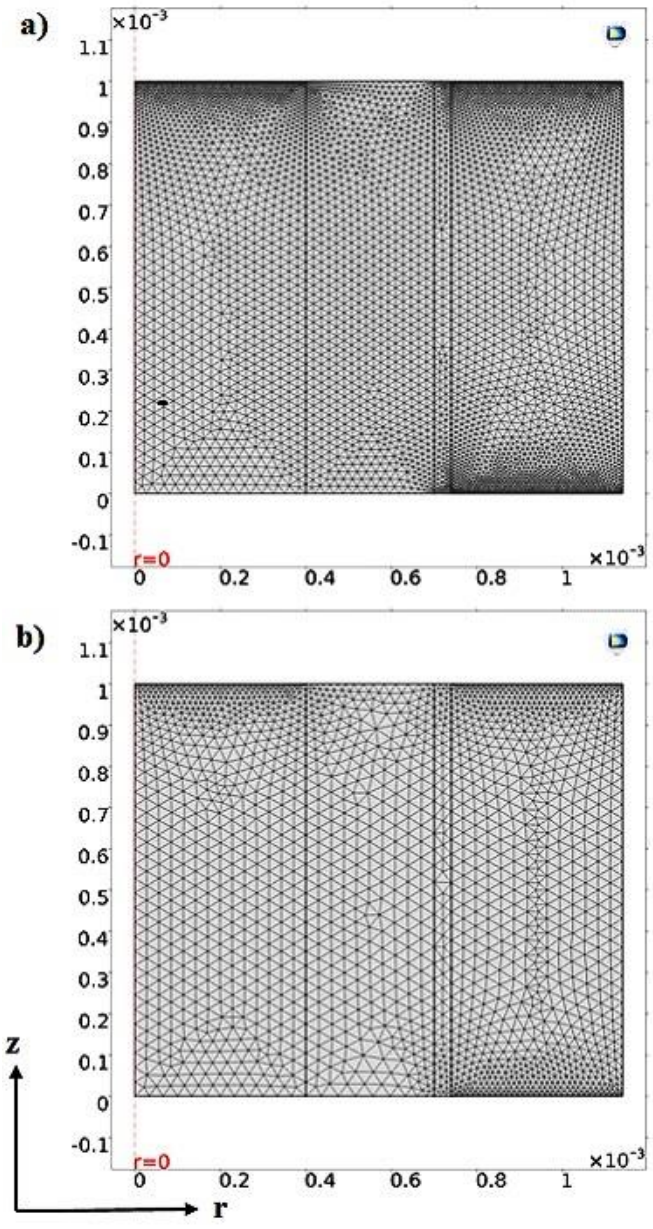

Fig. 3. The generated meshes in the model for (a) H_2, N_2, O_2 and He, (b) CO_2 and CH_4.

provided and the polymer chains become more flexible [67]. In this case, more free volume fractions for gas transport through the membrane are created. Furthermore, with increasing temperature, the mobility of the gas molecules will increase. This condition makes the gas components can diffuse more easily through the membrane and subsequently the permeability is increased [68].

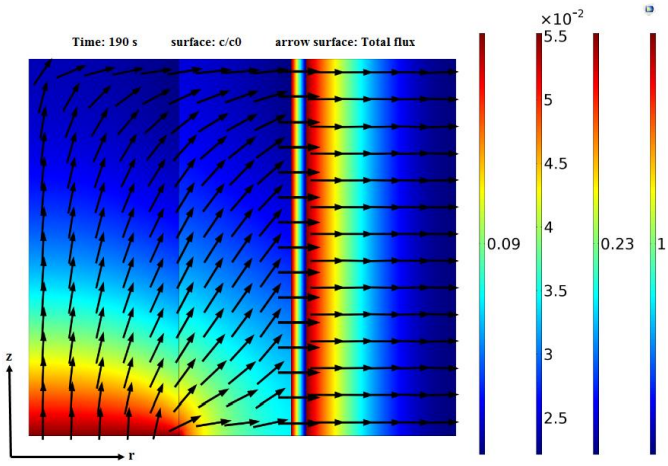

Fig. 4. The concentration gradient of N_2 and the total flux vectors in the model sections at P = 1 bar and T = 25 °C.

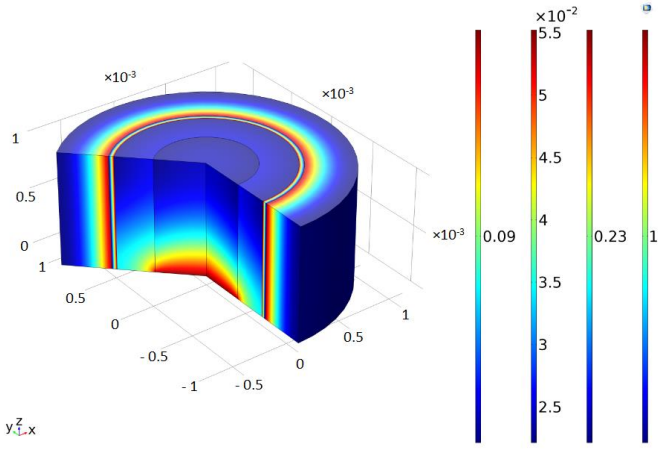

Fig. 5. The 2D axisymmetric concentration gradient of N_2 in various sections of the model at P = 1 bar and T = 25 °C.

4. Results and discussion

4.1. The concentration gradient of gas in the membrane model

Figures 4 and 5 depict the gas concentration gradient in the model sections. Figure 4 shows a 2D concentration gradient with total flux vectors of N_2. In addition, a 3D concentration gradient of N_2 is also presented in Figure 5, just for a better visualization of mass transfer. The feed gas enters at z = 0 and due to their concentration gradient is transferred through the model sections in the radial direction. The gas concentration decreases from feed to permeate sections. The governing mechanism in feed and permeate sections is diffusion and convection, while in the dense membrane, diffusion is the dominant mass transfer mechanism because of the low contribution of velocity.

4.2. Effect of temperature on gas permeability and solubility

Figures 6 and 7 show the effect of temperature on the gas permeability and solubility at the temperature range of 25-75 °C. As can be observed, with increasing the temperature, the permeability of gases increases while the solubility decreases. At higher temperatures, enough energy to overcome the interaction forces between the polymer chains in the membrane matrix is

Increasing permeability and decreasing solubility with the temperature increase for heavier gas components, such as CO_2, is significantly higher than of lighter ones. The effect of temperature on the permeability and solubility is justified by Van't Hoff–Arrhenius equations (Eqs. (40-42)) [69, 70].

$$P = P_0 \exp\left(\frac{-E_p}{RT}\right) \quad (40)$$

$$S = S_0 \exp\left(\frac{-\Delta H_s}{RT}\right) \quad (41)$$

$$D = D_0 \exp\left(\frac{-E_d}{RT}\right) \quad (42)$$

where E_p (kJ/mol) and ΔH_s (kJ/mol) refer to the activation energy of permeation and the enthalpy of sorption, respectively. Also, E_d (kJ/mol) is the activation energy of diffusion. Due to the difference in E_p and ΔH_s for various gas components, temperature has different effects on their permeability and solubility.

As can be seen in Figures 6 and 7, the same results are obtained in accordance with Van't Hoff–Arrhenius equations [69, 70]. That is, with increasing temperature, the permeability and solubility are increased and decreased respectively.

4.3. Effect of temperature on diffusion coefficient and time lag value

Figure 8 illustrates the effect of temperature on diffusion coefficient of gases in the membrane at temperature range of 25-75 °C. The diffusion coefficient of all gases increases with increasing temperature. Due to the difference in activation energies of diffusion, the effect of temperature on the diffusion coefficient of lighter gases such as H_2 is higher than of heavier ones. As described above, the flexibility of polymer chains increases with increasing the temperature, and therefore the diffusion coefficient increases. This behavior can be justified by Van't Hoff–Arrhenius equations (refer to Eq. (42)) [71, 72].

Due to the high solubility of gas components in rubbery membranes, direct predicting the diffusion time lag is complicated. In permeability measurements of a gas in rubbery polymers, the p-t curve shift to its steady state, and hence, it is almost hard-measurable the exact time of unsteady behavior in the beginning of experiment and the probable measured values can be along with a number of errors. To overcome the problem, the Frisch method is considered to calculate the diffusion coefficient and time lag values. The results of calculations through the method are presented in Table 1. As seen, by increasing the temperature, the time lag values decrease, in accordance well with the increase in diffusion coefficient and gas flux [28, 73, 74].

4.4. Model Validation

The model equations are solved for all four sections at a temperature range of 25-75 °C. In order to validate the model for verifying the accuracy of the obtained results, the model results are compared with the experimental data [27]. Table 2 shows the results of comparison for permeability, solubility, diffusion coefficient and selectivity of the model for H_2, O_2, N_2, CH_4, CO_2 and He. As can be seen, there is good conformity between the model results and experimental data with the maximum relative errors of 5.5, 4.5 and 9% respectively for the predictions of permeability, diffusion coefficient and solubility. The relative error is calculated by Eq. (43) [75]:

$$RE(\%) = \frac{|\text{simulation value - experimental value}|}{\text{experimental value}} \times 100 \quad (43)$$

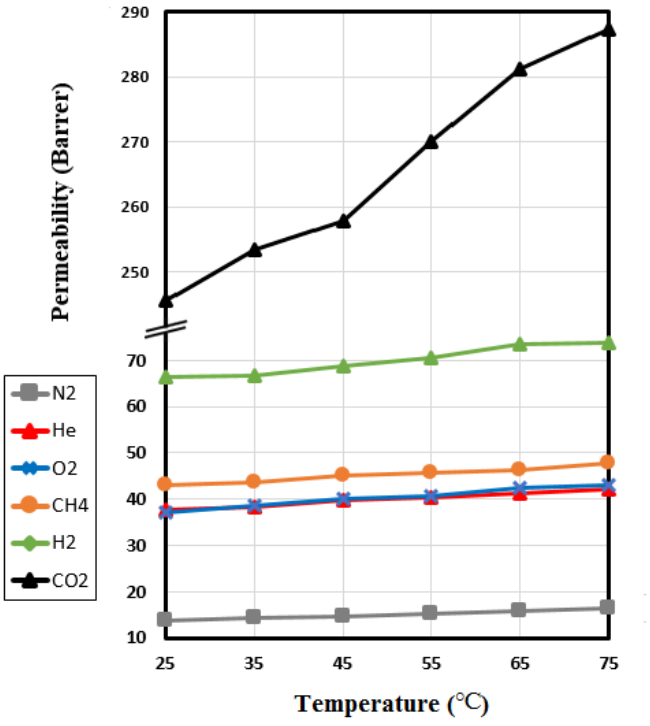

Fig. 6. Effect of temperature on gas permeability at P = 1 bar and membrane thickness of l = 40 μm.

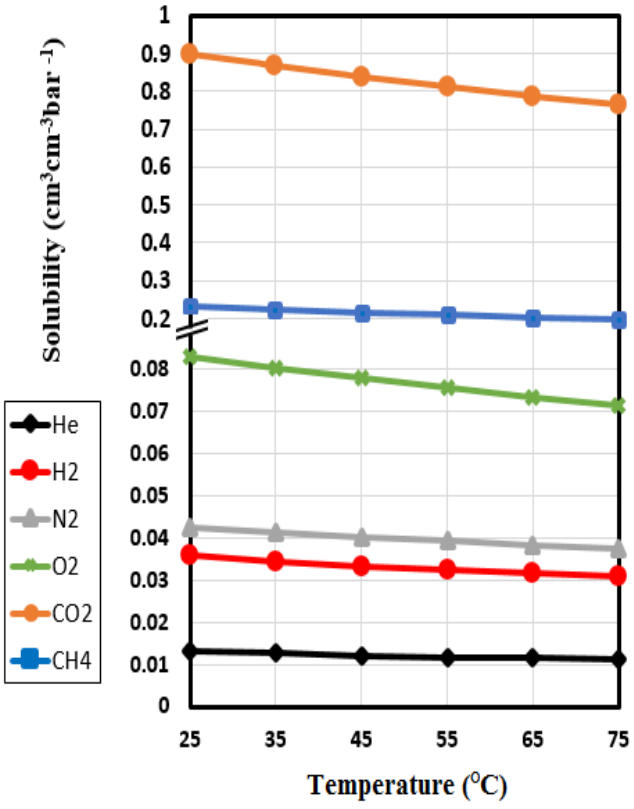

Fig. 7. Effect of temperature on gas solubility at P = 1 bar and membrane thickness of l = 40 μm.

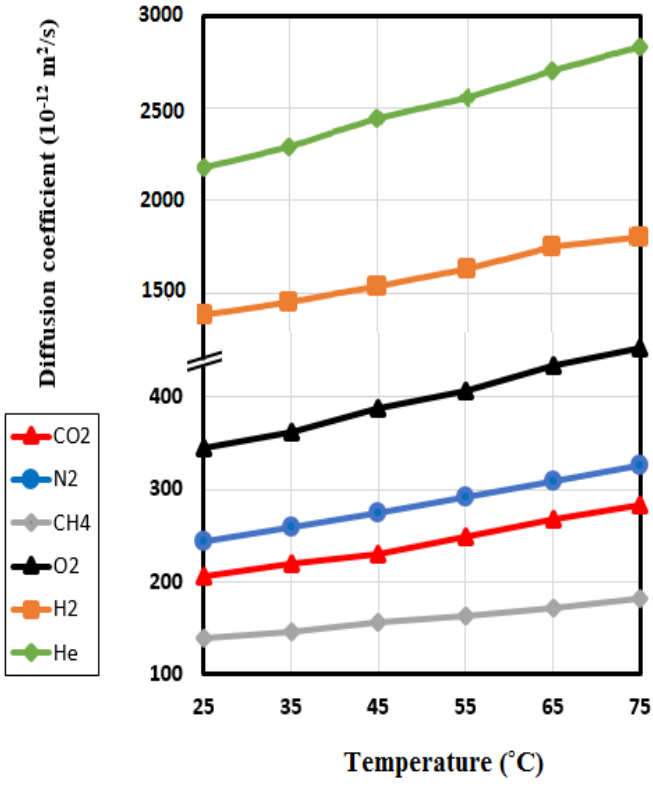

Fig. 8. Effect of temperature on the diffusion coefficients of gases in the membrane at P = 1 bar and membrane thickness of l = 40 μm.

Table 1
Time lag values obtained from the model at various temperatures.

Penetrate	Temperature (°C)					
	25	35	45	55	65	75
CH_4	1.85	1.83	1.70	1.63	1.56	1.46
CO_2	1.23	1.20	1.14	1.06	0.98	0.93
N_2	1.04	1.01	0.96	0.90	0.85	0.80
O_2	0.73	0.71	0.67	0.64	0.60	0.57
H_2	0.20	0.18	0.17	0.16	0.15	0.13
He	0.12	0.116	0.11	0.10	0.098	0.094

Table 2
Comparison of the model results with experimental data at 1 bar and 25 °C.

Gas Component	Presented study			Experimental Data			Ideal selectivity Gas/N_2	Relative error of permeability (%)	Relative error of diffusion coefficient (%)	Relative error of solubility (%)
	P (Barrer)	D×10^{-12} (m^2/s)	S (cm^3/(cm^3bar))	P (Barrer)	D×10^{-12} (m^2/s)	S (cm^3/(cm^3bar))				
CO_2	245.7	214.3	0.856	248	205	0.907	17.87	0.93	4.53	5.62
H_2	66.4	1350.3	0.0367	66	1380	0.036	4.83	0.6	2.15	1.94
CH_4	43	134.5	0.239	44	139	0.24	3.13	2.27	3.24	0.42
He	37.67	2151.3	0.0131	39	2180	0.013	2.74	3.4	1.32	0.77
O_2	38	358.5	0.079	36	344	0.078	2.76	5.55	4.21	1.28
N_2	13.75	252.3	0.04	14	243	0.044	-	1.78	3.83	9.1

5. Conclusions

A 2D model for determination of pure gas permeation properties through a hollow fiber composite membrane was developed. A hollow fiber type membrane module with four zones of feed, support, dense membrane and permeate was considered to modeling the transport phenomena. Unlike the composite membrane models, in this model the porous support was subjected to the feed gas and the dense membrane layer was located in the permeate side. The gas permeation of various pure gas components such as H_2, O_2, N_2, CH_4, CO_2 and He are calculated. The permeation results from the model had good conformity with experimental outcomes. Moreover, the effect of temperature on the effective parameters on the model performance was investigated. The obtained results indicated that with increasing the temperature, the permeability and the diffusion coefficient of the pure gas components are increased while their solubility decreased.

Nomenclatures

$C_{i,j}$	Concentration of species i in zone j (mole/ m^3)
D_i	Diffusion coefficient of species i (m^2/s)
E_d	Activation energies of diffusion (kJ/mol)
E_p	Activation energy of permeation (kJ/mol)
J	Gas diffusive flux ((mol/(m^2.s)
K	Partition coefficient (-)
L	Length of the fiber (mm)
L	Membrane thickness (mm)
M	Stiff-spring constant (-)
N	Total gas flux (mol/(m^2.s))
P	Pressure (bar)
P	Permeability (Barrer: 10^{-10} cm^3(STP)cm/(cm^2.s.cmHg))
R	The universal gas constant (J/(mol.K))
R	Radial coordinate (m)
S	Solubility constant (cm^3/(cm^3.bar^1))
T	Temperature (°C)
T	Time (s)
U	Velocity (m/s)
Z	Axial coordinate (mm)
Y	Axial coordinate (mm)

Greek letters

H	Viscosity (Pa.s)
P	Density (kg/ m^3)
∇	Gradient
α	selectivity (-)
θ	Time lag (s)

Subscript

0	Initial condition
1	Feed side
2	Support layer
3	Dense membrane
4	Permeate side
eff	Effective
f	Feed
i	Species i
j	Zone j
m	Membrane
p	Permeate
s	Support layer

Abbreviations

CO_2	Carbon dioxide
CH_4	Methane
D	Dimensional
Exp	Experimental
H_2	Hydrogen
He	Helium
N_2	Nitrogen
O_2	Oxygen
RE	Relative error
Sim	Simulation

References

[1] A. Ebadi Amooghin, H. Sanaeepur, M. Zamani Pedram, M. Omidkhah, A. Kargari, New advances in polymeric membranes for CO_2 separation, in: A. Méndez-Vilas, A. Solano-Martín (Eds.) Polymer science: research advances, practical applications and educational aspects, Formatex Research Center, Badajoz, Spain, 2016, pp. 354-368.

[2] H. Sanaeepur, R. Ahmadi, A. Ebadi Amooghin, D. Ghanbari, A novel ternary mixed matrix membrane containing glycerol-modified poly(ether-block-amide) (Pebax 1657)/copper nanoparticles for CO_2 separation, J. Membr. Sci. 573 (2019) 234-246.

[3] H. Sanaeepur, A. Ebadi Amooghin, E. Khademian, A. Kargari, M. Omidkhah, Gas permeation modeling of mixed matrix membranes: Adsorption isotherms and permeability models, Polym. Compos. 39 (2018) 4560-4568.

[4] M. Rezakazemi, A. Ebadi Amooghin, M.M. Montazer-Rahmati, A.F. Ismail, T. Matsuura, State-of-the-art membrane based CO_2 separation using mixed matrix membranes (MMMs): an overview on current status and future directions, Prog. Polym. Sci. 39 (2014) 817-861.

[5] A. Ebadi Amooghin, M. Omidkhah, A. Kargari, Enhanced CO_2 transport properties of membranes by embedding nano-porous zeolite particles into Matrimid®5218 matrix, RSC Advances, 5 (2015) 8552-8565.

[6] S. Sanaeepur, H. Sanaeepur, A. Kargari, M.H. Habibi, Renewable energies: climate-change mitigation and international climate policy, Int. J. Sustainable Energy. 33 (2014) 203-212.

[7] A. Ebadi Amooghin, M.M. Moftakhari Sharifzadeh, M. Zamani Pedram, Rigorous modeling of gas permeation behavior in facilitated transport membranes (FTMs); evaluation of carrier saturation effects and double-reaction mechanism, Greenh. Gas. Sci. Technol. 8 (2018) 429-443.

[8] S. Masoumi, P. Keshavarz, Z. Rastgoo, Theoretical investigation on CO_2 absorption into DEAB solution using hollow fiber membrane contactors, J. Nat. Gas Sci. Eng. 18 (2014) 23-30.

[9] M.R. Sohrabi, A. Marjani, S. Moradi, M. Davallo, S. Shirazian, Mathematical modeling and numerical simulation of CO_2 transport through hollow-fiber membranes, Appl. Math. Model. 35 (2011) 174-188.

[10] Z. Zhang, Y. Yan, L. Zhang, S. Ju, Numerical Simulation and Analysis of CO_2 Removal in a Polypropylene Hollow Fiber Membrane Contactor, Int. J. Chem. Eng. 2014 (2014) 7.

[11] M.M. Moftakhari Sharifzadeh, M. Zamani Pedram, A. Ebadi Amooghin, A new permeation model in porous filler–based mixed matrix membranes for CO_2 separation, Greenh. Gas. Sci. Technol. 9 (2019) 1-24.

[12] A. Ebadi Amooghin, S. Mashhadikhan, H. Sanaeepur, A. Moghadassi, T. Matsuura, S. Ramakrishna, Substantial breakthroughs on function-led design of advanced materials used in mixed matrix membranes (MMMs): A new horizon for efficient CO_2 separation, Prog. Mater. Sci. 102 (2019) 222-295.

[13] H. Sanaeepur, A. Ebadi Amooghin, S. Bandehali, Theoretical gas permeation models for mixed matrix membranes, LAP LAMBERT Academic Publishing, ISBN: 978-613-9-86189-7, June (2018).

[14] A. Ebadi Amooghin, H. Sanaeepur, M. Omidkhah, A. Kargari, "Ship-in-a-bottle", a new synthesis strategy for preparing novel hybrid host–guest nanocomposites for highly selective membrane gas separation, J. Mater. Chem. A. 6 (2018) 1751-1771

[15] H. Sanaeepur, A. Ebadi Amooghin, S. Bandehali, A. Moghadassi, T. Matsuura, B. Van der Bruggen, Polyimides in membrane gas separation: Monomer's molecular design and structural engineering, Prog. Polym. Sci. 91 (2019) 80-125.

[16] S.M. Nowee, M. Taherian, M. Salimi, S.M. Mousavi, Modeling and simulation of phenol removal from wastewater using a membrane contactor as a bioreactor, Appl. Math. Model. 42 (2017) 300-314.

[17] Z. Qi, E.L. Cussler, Microporous hollow fibers for gas absorption: II. Mass transfer across the membrane, J. Membr. Sci. 23 (1985) 333-345.

[18] A. Ebadi Amooghin, P. Moradi Shehni, A. Ghadimi, M. Sadrzadeh, T. Mohammadi, Mathematical modeling of mass transfer in multicomponent gas mixture across the synthesized composite polymeric membrane, J. Ind. Eng. Chem. 19 (2013) 870-885.

[19] M. Darabi, M. Rahimi, A.M. Dehkordi, Gas absorption enhancement in hollow fiber membrane contactors using nanofluids: Modeling and simulation, Chem. Eng. Process 119 (2017) 7-15.

[20] S.S. Hosseini, J.A. Dehkordi, P.K. Kundu, Mathematical modeling and investigation on the temperature and pressure dependency of permeation and membrane separation performance for natural gas treatment, Chem. Prod. Process Model. 11 (2016) 7-10.

[21] M. Farjami, A. Moghadassi, V. Vatanpour, Modeling and simulation of CO_2 removal in a polyvinylidene fluoride hollow fiber membrane contactor with computational fluid dynamics, Chem. Eng. Process 98 (2015) 41-51.

[22] P. Tantikhajorngosol, N. Laosiripojana, R. Jiraratananon, S. Assabumrungrat, Physical absorption of CO_2 and H_2S from synthetic biogas at elevated pressures using hollow fiber membrane contactors: The effects of Henry's constants and gas diffusivities, Int. J. Heat Mass Transfer. 128 (2019) 1136-1148.

[23] A. Azari, M.A. Abbasi, H. Sanaeepur, CFD study of CO_2 separation in an HFMC: Under non-wetted and partially-wetted conditions, Int. J. Greenh. Gas Control. 49 (2016) 81-93.

[24] M.R. Talaghat, A.R. Bahmani, Mathematical modeling of carbon dioxide removal from the CO_2/CH_4 gas mixture using amines and blend of amines in polypropylene: A comparison between hollow fiber membrane contactor and other membranes, J. Pet. Sci. Technol. 7 (2017) 41-53.

[25] J.A. Dehkordi, S.S. Hosseini, P.K. Kundu, N.R. Tan, Mathematical modeling of natural gas separation using hollow fiber membrane modules by application of finite element method through statistical analysis, Chem. Prod. Process Model. 11 (2016) 11-15.

[26] M.M. Moftakhari Sharifzadeh, A. Ebadi Amooghin, M. Zamani Pedram, M. Omidkhah, Time-dependent mathematical modeling of binary gas mixture in facilitated transport membranes (FTMs): A real condition for single-reaction mechanism, J. Ind. Eng. Chem. 39 (2016) 48-65.

[27] F. Bazzarelli, P. Bernardo, F. Tasselli, G. Clarizia, V.G. Dzyubenko, P. Vdovin, J.C. Jansen, Multilayer composite SBS membranes for pervaporation and gas separation, Sep. Purif. Technol. 80 (2011) 635-642.

[28] P. Moradi Shehni, A. Ebadi Amooghin, A. Ghadimi, M. Sadrzadeh, T. Mohammadi, Modeling of unsteady-state permeation of gas mixture through a self-synthesized PDMS membranes, Sep. Purif. Technol. 76 (2011) 385-399.

[29] A. Ebadi Amooghin, H. Sanaeepur, A. Kargari, A. Moghadassi, Direct determination of concentration-dependent diffusion coefficient in polymeric membranes based on the Frisch method, Sep. Purif. Technol. 82 (2011) 102-113.

[30] X. Hu, J. Tang, A. Blasig, Y. Shen, M. Radosz, CO_2 permeability, diffusivity and solubility in polyethylene glycol-grafted polyionic membranes and their CO_2 selectivity relative to methane and nitrogen, J. Membr. Sci. 281 (2006) 130-138.

[31] R. Bird, W. Stewart, E. Lightfoot, Transport Phenomena 2nd ed., John Wiley & Sons, New York, 2007.

[32] M. Rezakazemi, S. Shirazian, S.N. Ashrafizadeh, Simulation of ammonia removal from industrial wastewater streams by means of a hollow-fiber membrane contactor, Desalination, 285 (2012) 383-392.

[33] M. Rezakazemi, Z. Niazi, M. Mirfendereski, S. Shirazian, T. Mohammadi, A. Pak, CFD simulation of natural gas sweetening in a gas–liquid hollow-fiber membrane contactor, Chem. Eng. J. 168 (2011) 1217-1226.

[34] H. Sanaeepur, O. Hosseinkhani, A. Kargari, A. Ebadi Amooghin, A. Raisi, Mathematical modeling of a time-dependent extractive membrane bioreactor for denitrification of drinking water, Desalination, 289 (2012) 58-65.

[35] N. Ghasem, M. Al-Marzouqi, Modeling and Experimental Study of Carbon Dioxide Absorption in a Flat Sheet Membrane Contactor, J. Membr. Sci. Res. 3 (2017) 57-63.

[36] J. Happel, Viscous flow relative to arrays of cylinders, AIChE J. 5 (1959) 174-177.

[37] W.M. Clark, COMSOL multiphysics models for teaching chemical engineering fundamentals: absorption column models and illustration of the two-film theory of mass transfer, in: COMSOL Conference, Boston, 2008.

[38] V.S.J. Craig, B.W. Ninham, R.M. Pashley, Direct measurement of hydrophobic forces: A study of dissolved gas, approach rate, and neutron Irradiation, Langmuir, 15 (1999) 1562-1569.

[39] P. Buchwald, Exploratory FEM-based multiphysics oxygen transport and cell viability models for isolated pancreatic islets, in: Proceedings of the COMSOL Conference 2008 Boston, Comsol, Inc., Boston, 2008.

[40] J. Lebowitz, W. Clark, Gas permeation laboratory experiment simulation for improved learning, in: COMSOL Conference, Boston, 2006.

[41] Comsol, AB COMSOL Multiphysics Chemical Engineering Module Model Library, version 4.4, COMSOL AB (2007).

[42] M. Sadrzadeh, K. Shahidi, T. Mohammadi, Effect of operating parameters on pure and mixed gas permeation properties of a synthesized composite PDMS/PA membrane, J. Membr. Sci. 342 (2009) 327-340.

[43] K. Ghosal, B.D. Freeman, Gas separation using polymer membranes: an overview, Polym. Adv. Technol. 5 (1994) 673-697.

[44] A. Ghadimi, M. Sadrzadeh, K. Shahidi, T. Mohammadi, Ternary gas permeation through a synthesized PDMS membrane: Experimental and modeling, J. Membr. Sci. 344 (2009) 225-236.

[45] A. Ebadi Amooghin, H. Sanaeepur, A. Moghadassi, A. Kargari, D. Ghanbari, Z.S. Mehrabadi, Modification of ABS Membrane by PEG for Capturing Carbon Dioxide from CO_2/N_2 Streams, Sep. Sci. Technol. 45 (2010) 1385-1394.

[46] H. Sanaeepur, A. Ebadi Amooghin, A. Kargari, M. Omidkhah, A. Ismail, S. Ramakrishna, Interior Modification of Nano-Porous Fillers to Fabricate High-Performance Mixed Matrix Membranes, IJChE. 16 (2019) 71.

[47] H. Sanaeepur, A. Ebadi Amooghin, A. Moghadassi, A. Kargari, Preparation and characterization of acrylonitrile–butadiene–styrene/poly(vinyl acetate) membrane for CO_2 removal, Sep. Purif. Technol. 80 (2011) 499-508.

[48] F. Ranjbaran, M. Omidkhah, A. Ebadi Amooghin, The novel Elvaloy4170/functionalized multi-walled carbon nanotubes mixed matrix membranes: Fabrication, characterization and gas separation study, J. Taiwan Inst. Chem. Eng. 49 (2015) 220-228.

[49] W.H. Lin, R.H. Vora, T.-S. Chung, Gas transport properties of 6FDA-durene/1,4-phenylenediamine (pPDA) copolyimides, J. Polym. Sci. 38 (2000) 2703-2713.

[50] K. Wang, H. Suda, K. Haraya, Permeation Time Lag and the Concentration Dependence of the Diffusion Coefficient of CO_2 in a Carbon Molecular Sieve Membrane, Ind. Eng. Chem. Res. 40 (2001) 2942-2946.

[51] H. Wu, B. Kruczek, J. Thibault, Impact of Measuring Devices and Data Analysis on the Determination of Gas Membrane Properties, J. Membr. Sci. Res. 4 (2018) 4-14.

[52] J. Petropoulos, P. Roussis, Permeation time-lag analysis of anomalous diffusion: part 2, J. Chem. Soc. Faraday Trans. II, 37 (1977) 1025.

[53] H.L. Frisch, Anomalous polymer-penetrant permeation, J. Chem. Phys. 37 (1962) 2408-2413.

[54] J. Crank, Diffusion in a plane sheet. The mathematics of diffusion, 2nd ed., Oxford University Press, London, 1975.

[55] R.A. Siegel, E.L. Cussler, Reactive barrier membranes: some theoretical observations regarding the time lag and breakthrough curves, J. Membr. Sci. 229 (2004) 33-41.

[56] E. Favre, N. Morliere, D. Roizard, Experimental evidence and implications of an imperfect upstream pressure step for the time-lag technique, J. Membr. Sci. 207 (2002) 59-72.

[57] R. Ash, S.E. Espenhahn, D.E.G. Whiting, Transport through a slab membrane governed by a concentration-dependent diffusion coefficient: Part II. The four time-lags for some particular D(C), J. Membr. Sci. 166 (2000) 281-301.

[58] A. Strzelewicz, Z.J. Grzywna, On the permeation time lag for different transport equations by Frisch method, J. Membr. Sci. 322 (2008) 460-465.

[59] W.H. Lin, R.H. Vora, T.S. Chung, Gas transport properties of 6FDA-durene/1, 4-phenylenediamine (pPDA) copolyimides, J. Polym. Sci. 38 (2000) 2703-2713.

[60] X.Q. Nguyen, Z. Brož, P. Uchytil, Q.T. Nguyen, Methods for the determination of transport parameters of gases in membranes, J. Chem. Soc., Faraday Trans. 88 (1992) 3553-3560.

[61] A. Ghadimi, M. Sadrzadeh, T. Mohammadi, Prediction of ternary gas permeation through synthesized PDMS membranes by using Principal Component Analysis (PCA) and fuzzy logic (FL), J. Membr. Sci. 360 (2010) 509-521.

[62] M. Sadrzadeh, E. Saljoughi, K. Shahidi, T. Mohammadi, Preparation and characterization of a composite PDMS membrane on CA support, Polym.Adv. Technol. 21 (2010) 568-577.

[63] E. Ghasemi Estahbanati, M. Omidkhah, A. Ebadi Amooghin, Interfacial design of ternary mixed matrix membranes containing Pebax 1657/silver-nanopowder/[BMIM][BF_4] for improved CO_2 separation performance, ACS Appl. Mater. Interfaces. 9 (2017) 10094-10105.

[64] A. Ebadi Amooghin, S. Jafari, H. Sanaeepur, A. Kargari, Computational fluid dynamics simulation of bubble coalescence and breakup in an internal airlift reactor: analysis of effects of a draft tube on hydrodynamics and mass transfer, Appl. Math. Model. 39 (2015) 1616-1642.

[65] A. Hekmat, A. Ebadi Amooghin, M.K. Moraveji, CFD simulation of gas–liquid flow behaviour in an air-lift reactor: determination of the optimum distance of the draft tube, Simul. Model. Pract. Th. 18 (2010) 927-945.

[66] C.R. Wilke, C.Y. Lee, Estimation of diffusion coefficients for gases and vapors, Ind. Eng. Chem. 47 (1955) 1253-1257.

[67] A. Ebadi Amooghin, M. Omidkhah, A. Kargari, The effects of aminosilane grafting on NaY zeolite–Matrimid® 5218 mixed matrix membranes for CO_2/CH_4 separation, J. Membr. Sci. 490 (2015) 364-379.

[68] P. Guan, J. Luo, W. Li, Z. Si, Enhancement of gas permeability for CH_4/N_2 separation membranes by blending SBS to Pebax polymers, Macromol. Res. 25 (2017) 1007-1014.

[69] R.D. Raharjo, B.D. Freeman, D.R. Paul, G.C. Sarti, E.S. Sanders, Pure and mixed gas CH_4 and n-C_4H_{10} permeability and diffusivity in poly(dimethylsiloxane), J. Membr. Sci. 306 (2007) 75-92.

[70] T.C. Merkel, R.P. Gupta, B.S. Turk, B.D. Freeman, Mixed-gas permeation of syngas components in poly(dimethylsiloxane) and poly(1-trimethylsilyl-1-propyne) at elevated temperatures, J. Membr. Sci. 191 (2001) 85-94.

[71] R.S. Prabhakar, T.C. Merkel, B.D. Freeman, T. Imizu, A. Higuchi, Sorption and Transport Properties of Propane and Perfluoropropane in Poly(dimethylsiloxane) and Poly(1-trimethylsilyl-1-propyne), Macromolecules, 38 (2005) 1899-1910.

[72] G. Clarizia, C. Algieri, E. Drioli, Filler-polymer combination: a route to modify gas transport properties of a polymeric membrane, Polymer, 45 (2004) 5671-5681.

[73] C. Yeom, S. Lee, H. Song, J. Lee, Vapor permeations of a series of VOCs/N_2 mixtures through PDMS membrane, J. Membr. Sci. 198 (2002) 129-143.

[74] V. Shah, B. Hardy, S. Stern, Solubility of carbon dioxide, methane, and propane in silicone polymers: effect of polymer side chains, J. Polym. Sci., Part B: Polym. Phys. 24 (1986) 2033-2047.

[75] A. Ebadi Amooghin, M. Lashani, M.M. Moftakhari Sharifzadeh, H. Sanaeepur, A novel analytical method for prediction of gas permeation properties in ternary mixed matrix membranes: Considering an adsorption zone around the particles, Sep. Purif. Technol. 225 (2019) 112-128.